Photoelectrochemical Studies of MoS_2 Electrode by Rotating Ring-disk Electrode Technique

Akira Fujishima,* Yoshikazu Noguchi, Kenichi Honda, and Boon H. Loo†

Department of Synthetic Chemistry, Faculty of Engineering, The University of Tokyo, Hongo, Bunkyo-ku, Tokyo 113

† *Materials Research Laboratory, SRI International, Menlo Park, California 94025, U. S. A.*

(Received February 4, 1981)

Photoelectrochemical processes at both n- and p-type MoS_2 electrodes were studied by rotating ring-disk electrode technique. In comparison with other semiconductor photoelectrodes such as CdS, ZnO, and TiO_2, the competitive oxidations of various reducing agents at n-MoS_2 electrode were not clearly dependent on their redox potentials. The MoS_2 photoanode was particularly stabilized in I^- solutions, and this was attributed to the specific adsorption of I^- ions on the electrode surface. Two step waves were observed in the photocurrent-potential curves of MoS_2 photoanode in I^- solutions. The first wave was controlled by the diffusion of I^- ions from the bulk solution to the electrode surface, and the second wave at more anodic potential was dependent on the formation of the photogenerated holes.

There are about sixty kinds of transition metal dichalcogenides, and approximately 70% of them have two dimensional layer structures. This layer structure exerts great influence on the solid state properties of these dichalcogenides, in particular, the intercalation processes which have been investigated to achieve superconduction[1] and high current density batteries.[2]

Tributsch and his coworkers were the first to investigate the photoelectrochemical reactions at some layer-type semiconductor electrodes (MoS_2,[3,4] $MoSe_2$,[5,6] and WSe_2[7]). These layer type semiconductors are attractive materials for solar energy conversion because they have small bandgaps and an expected higher stability against photocorrosion, since their main photoelectrochemical reactions are based on holes from d-bands belonging to the non-bonding orbitals of the transition metals. Photoanodes using transition metal dichalcogenide semiconductor materials in photoelectrochemical cells have been reported by several groups.[3–23] Molybdenum dichalcogenide photoanodes were especially stabilized by I^-.[3–6] Electrochemical photocells based on n-WSe_2/I^- and n-$MoSe_2$/I^- systems have been reported recently to have solar conversion efficiencies of 10.2 and 9.4%, respectively.[23]

In this study we investigated in detail the photoelectrochemical processes which occurred at n-type and p-type MoS_2 electrodes by rotating ring-disk electrode (RRDE) technique, which is very useful to measure electrochemical products. Competitive reactions of I^- and other redox agents were studied to provide insights on the corrosion and stabilization processes.

Experimental

The MoS_2 single crystals (n- and p-type) used in the present study were produced naturally in Japan. The crystal was cleaved between layers and shaped into a disk of diameter 5.0 mm. Ohmic contact with a conducting wire was made by rubbing In–Ga alloy on one side of the crystal. The MoS_2 disk was then mounted on a Teflon holder using an epoxy resin with a Pt ring 7.0 mm in inner diameter and 9.0 mm in outer diameter. The MoS_2 (001) face exposed to the electrolyte was etched in 5 M HCl (1 M=1 mol dm^{-3}) for 30 s, and then rinsed with distilled water. The ring-disk electrode was set in a RRDE measurement system (Nikko Keisoku). The potentials of the disk and ring electrodes were controlled independently by means of a dual-potentiostat (Nikko Keisoku). The light source was a 250 W high pressure Hg lamp and the wavelength of illuminating light was selected with a V-Y44 (440 nm) cutoff filter (Toshiba Kasei). The rotation speed of the RRDE was set at 1000 min^{-1}. All chemicals used were of reagent grade. The experimental detail of the RRDE measurements was described elsewhere.[24]

Results and Discussion

Photoelectrochemical Reactions at an n-MoS_2 Electrode. The anodic reactions at an illuminated n-MoS_2 electrode in an inert electrolyte involved the following processes:[3]

$$MoS_2 + 8H_2O + 18h^+ \longrightarrow Mo(VI) + 2SO_4^{2-} + 16H^+, \quad (1)$$

$$MoS_2 + 4h^+ \longrightarrow Mo(IV) + 2S, \quad (2)$$

$$MoS_2 + 2H_2O + 4h^+ \longrightarrow MoS_2 + O_2 + 4H^+. \quad (3)$$

We performed quantitative analysis on all possible reaction products and found that Reaction 1 was the predominant process (Table 1), which agreed with Tributsch's results.[3] Our SEM experiments showed that elemental sulfur was present on the electrode surface in all cases. This suggests Reaction 2 always occurs to some extent in an inert electrolyte. Both Reactions 1 and 2 lead to the dissolution of the photoanode. Reaction 3 occurs in a smaller extent, however, it is the main focus of interest since water is splitted without degradation of the photoanode. Photocorrosion of MoS_2 electrode will be suppressed if Reactions 1 and 2 are suppressed.

Perhaps the photoanodic reactions at an n-MoS_2 electrode are analogous to those occuring at a pyrite (FeS_2) electrode, which has been investigated in detail by Biegler and Swift.[25] The anodic reactions at a pyrite electrode are composed of two processes which lead to formation of sulphate and elemental sulfur.

Flatband Potential of n-MoS_2 Electrode. We measured the flatband potential of n-MoS_2 electrode in 0.2 M Na_2SO_4 solution with variation in pH by impedance measurements. The flatband potential was

Table 1. Results of quantitative analysis of molybdenum ions and pH change

	Solution	Charge flowed Q	Amount of Mo[a] mg	Number of electrons or holes	pH change
Light (all wavelengths)	0.1 M KCl 150 ml	43.04	2.23	19.19	5.35→2.90
Monochromatic light (540 nm)	0.1 M KCl 150 ml	51.81	2.35	21.92	5.35→2.80
Monochromatic light (580 nm)	0.1 M KCl 100 ml	4.11	0.284	14.39	5.35→3.78

a) Colorimetric analysis of thiocyanate.

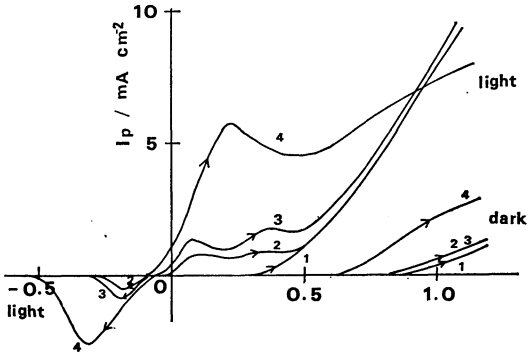

Fig. 1. Current-potential curves of n-MoS_2 electrode in 0.2 M Na_2SO_4 solutions with various concentrations of I^- ions.
1: 0 M, 2: 5×10^{-3} M, 3: 10^{-2} M, 4: 10^{-1} M.

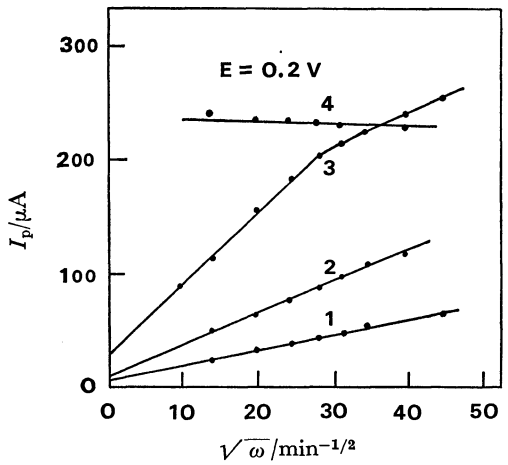

Fig. 2. Dependence of photocurrent at n-MoS_2 electrode on the rotating speed in 0.2 M Na_2SO_4 solutions with different concentrations of I^- ions.
1: 10^{-3} M, 2: 5×10^{-3} M, 3: 10^{-2} M, 4: 5×10^{-2} M.

found to be 0.15±0.05 V *vs.* SCE. This value agreed with those reported by others, 0.10 to 0.20 V in 1 M KCl aqueous electrolyte[6] and 0.30 V in CH_3CN.[17] Analogous to the behavior for CdS, the flatband potential of n-MoS_2 was found to be independent of the pH of the electrolyte. However, since the main photoanodic process of MoS_2 involved the reaction with water (Reaction 1 above), the onset of the photocurrent was influenced slightly by the variation of pH.

The donor concentration N_D of MoS_2 calculated by Mott-Schottky relationship was 1.3×10^{18} cm^{-3} (the dielectric constant of MoS_2: $\varepsilon=7$—8[26]). As the MoS_2 crystal used in the present study was a natural product, it might contain Si, Al, or Fe *etc.* as impurities.[27] Assuming much of the light was efficiently absorbed in the space charge region and using the relationship[28] $N_D=1.1\times10^{16}\times\Delta v\times a^2$, the voltage drop in the space charge layer Δv was 1.5 V, N_D being calculated donor density and a the absorption coefficient in the order of 10^{15} cm^{-1}.[27] This large drop in potential in the space charge region probably accounted for the slow rise in the photocurrent (see Fig. 1 curve 1).

The Behavior of n-MoS_2 Electrode in an I^--containing Electrolyte. Iodide ion effectively suppresses the anodic dissolution of n-MoS_2 and n-$MoSe_2$, and shifts the flatband potentials of the electrodes to more negative potentials.[5] Figure 1 shows the current-potential curves of MoS_2 photoanode in 0.2 M Na_2SO_4 solution containing different concentrations of I^- ions. The onset of the photocurrent was shifted to more negative potential as the I^- concentration increased. This shift in the onset of the photocurrent was due to a shift in the flatband potential. This behavior was quite similar to the two-step or three-step wave photocurrent observed at a CdS photoanode in a solution containing S^{2-}, SO_3^{2-}, or $S_2O_3^{2-}$ ions.[29,30] In our previous study of CdS–S^{2-} system,[29] we reported that the first wave was controlled by the diffusion of S^{2-} from the solution to the electrode surface and the second wave depended on the formation of the photoholes in the valence band.

We believed also the first wave (hereby referred to as region A) of the photocurrent-potential curve of n-MoS_2 in I^- solutions was due to the photo-oxidation of I^- ions, and was controlled by the diffusion of I^- ions from the solution to the electrode surface, and the second wave at more anodic potential (region B) was due to both the photo-oxidation of I^- ions and the photocorrosion of the electrode material, and would be dependent on the formation of the photogenerated holes in the valence band. To test our hypothesis, we studied the dependence of photocurrents on both the rotation speed and the illumination intensity. Figure 2 shows the photocurrent at region A was proportional to the square root of the rotation speed, this indicated that the rate-determining step was the diffusion of I^- from the solution to the electrode surface. Photocurrent at region B was found to be linearly dependent on the light intensity, irrespective of the I^- concentrations (Fig. 3(B)), this showed that the magnitude of the photocurrent at region B was determined by the amount of the photogenerated holes.

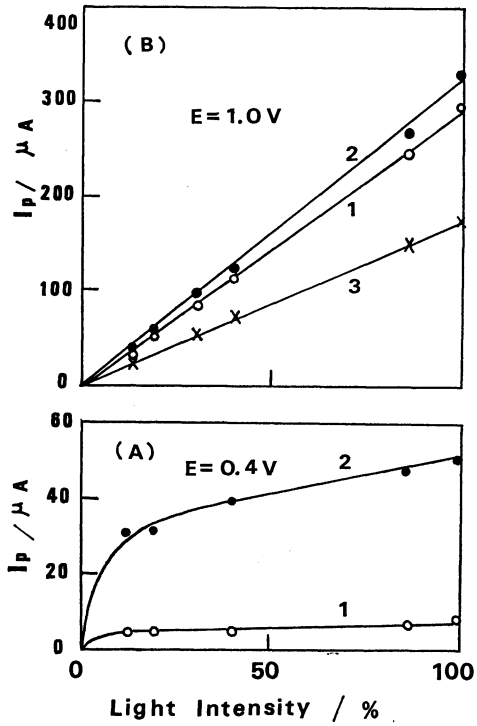

Fig. 3. Dependence of the photocurrent at n-MoS_2 electrode on the illumination intensity in 0.2 M Na_2SO_4 solutions with different concentrations of I^- ions at two different potentials. The rotation speed was 0 min^{-1}.
1: 10^{-3} M, 2: 10^{-2} M, 3: 10^{-1} M.

At region A, when I^- concentration was low ($<10^{-2}$ M) such that the duffusion process of I^- ions was important, the photocurrent was nearly independent of the light intensity (Fig. 3(A)).

Figure 4 shows the current-potential curves of Pt ring/n-MoS_2 disk RRDE. The potential of Pt ring (E_R) was held at 0 V *vs.* SCE to detect the current (I_R) due to the reduction of I_2 which was produced at the MoS_2 disk electrode. In the absence of I^-, no ring current could be observed (upper portion of Fig. 4, curve 1). This indicated that the current at the MoS_2 disk in the presence or absence of light (lower portion of Fig. 4, curve 1) was due to the dissolution of the MoS_2 electrode. Ring current was observed in the presence of I^- ions. At low E_D (<0.4 V), $-I_R/I_D$ was 0.2 which was the same as the collection efficiency of the present RRDE assembly. This meant at $E_D<0.4$ V, all of the photogenerated holes at the MoS_2 disk was totally consumed by the I^- ions, that is, the MoS_2 photoanode was 100% stabilized. At more anodic potentials, $-I_R/I_D$ was smaller than 0.2, and was significantly less than 0.2 at a lower I^- concentration. The ratio $-I_R/I_D$ describes the competitive hole capture by the I^- ions in solution (the stabilization process) and hole capture by surface atoms of the MoS_2 electrode (the corrosion process).

Figure 5 shows the ratio of the competitive hole capture by I^- ions to that by MoS_2 as a function of the I^- concentration. At $E=0.3$ V (in the region A referred to above), the ratio was 1 and was independent of the I^- concentration, since the photocurrent

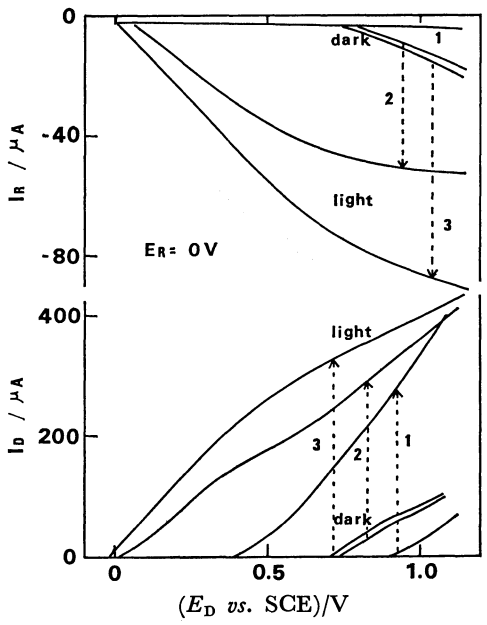

Fig. 4. I_R-E_D, I_D-E_D curves of Pt ring/n-MoS_2 disk electrode in 0.2 M Na_2SO_4 solutions with different concentrations of I^- ions. The rotation speed was 1000 min^{-1} and the scan rate was 30 s/V.
1: 0 M, 2: 2×10^{-3} M, 3: 10^{-2} M.

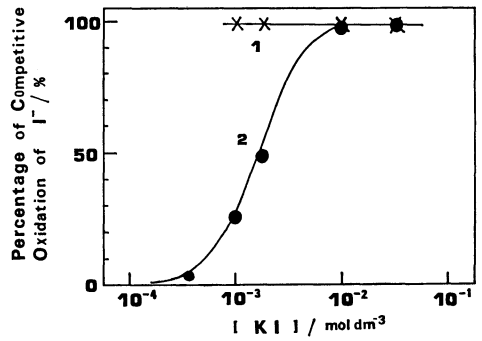

Fig. 5. Dependence of percentage of competitive reaction at n-MoS_2 electrode on concentration of I^- at two different potentials, and at constant light intensity, and rotation speed.
1: $E=0.3$ V, 2: 1.2 V.

was entirely due to the photo-oxidation of I^-. At more anodic potential (1.2 V), the photocurrent was due to the competitive hole capture by I^- and hole capture by MoS_2, thus the higher the I^- concentration, the larger was the ratio. Hole capture by the I^- ions was 100% when the I^- concentration was 10^{-2} M or higher.

The specific effect of I^- at the MoS_2 photoanode is similar to that of S^{2-} at the CdS photoanode.[24,32] The stabilization of the photoanode in I^- solutions may be attributed to the strong specific adsorption of I^- on the MoS_2 electrode surface, and the adsorption sites may act as surface states which participated in charge transfer.

Competitive Oxidations of Various Reducing Agents at n-MoS_2 Electrode. We reported earlier that, in the case of CdS,[24] ZnO,[31] and TiO_2,[32] the ratio of the competitive reaction increased as the redox

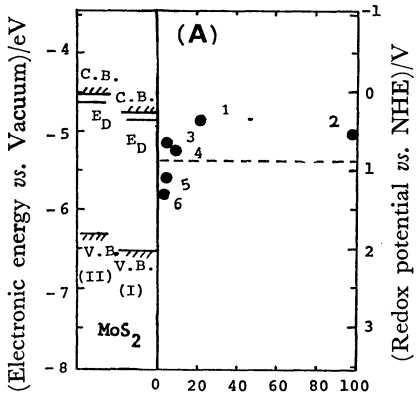

Fig. 6(A). Correlation between the energy diagram of MoS_2 and dependences of competitive ratios on redox potentials of reducing agents (0.01 M) at pH=6.
(I): Without I^-, (II): with I^-.
1: $Fe(CN)_6^{3-/4-}$, 2: I^-/I_2, 3: H_2Q/Q, 4: $Fe^{2+/3+}$, 5: Br^-/Br_2, 6: Cl^-/Cl_2.
---: Oxidation potential of water.

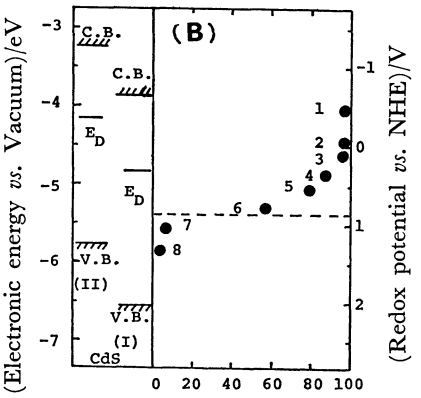

Fig. 6(B). Correlation between the energy diagram of CdS and dependences of competitive ratios on redox potentials of reducing agents (0.01 M) at pH=6.
(I): Without S^{2-}, (II): with S^{2-}.
1: S^{2-}/S, 2: $S_2O_3^{2-}/S_4O_6^{2-}$, 3: $SO_3^{2-}/S_2O_6^{2-}$, 4: $Fe(CN)_6^{4-/3-}$, 5: I^-/I_2, 6: $Fe^{2+/3+}$, 7: Br^-/Br_2, 8: Cl^-/Cl_2.
----: Oxidation potential of water.

potential of the reducing agent became more negative. Figure 6(A) shows the ratios of the competitive reactions of various reducing agents at the n-MoS_2 electrode as a function of their redox potentials, as compared to that at the CdS electrode (Fig. 6(B)). The oxidation potentials E_D of MoS_2 and CdS were derived from the thermodynamic data. The ratios of the competitive oxidation of the various reducing agents except I^- at the n-MoS_2 electrode were very small, indicating that these reducing agents were not suitable for the stabilization of the MoS_2 photoanode. Additionally, the competitive oxidations of the reducing agents were not clearly dependent on their redox potentials.

Photoanodic Reactions at n-MoS_2 Electrode in a Non-aqueous Solvent. We also investigated the photo-

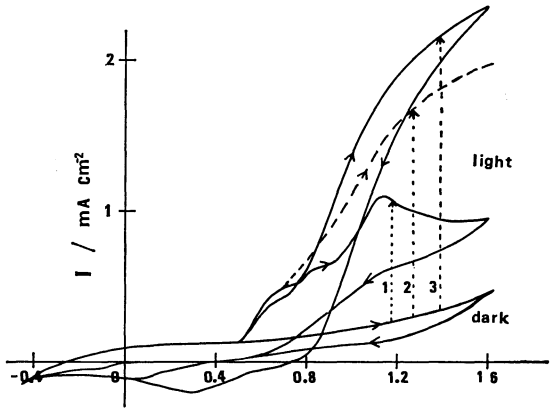

Fig. 7. *I-E* curves of n-MoS_2 in CH_3CN+0.1 M $NaClO_4$. The sweep rate was 10 s/V.
1: 1.4×10^{-3} M $I^-+1.4\times10^{-3}$ M H_2Q, no stirring,
2: 1.4×10^{-3} M $I^-+1.4\times10^{-3}$ M H_2Q, stirring, 3: 1.4×10^{-3} M I^-+10^{-2} M H_2Q, no stirring.

anodic reactions at the n-MoS_2 electrode in a non-aqueous solvent CH_3CN containing I^- and H_2Q (hydroquinine). In the presence of equal concentrations of I^- and H_2Q, some peaks could be observed (Fig. 7, curve 1), which were not seen in CH_3CN containing I^- and H_2Q individually. When excess H_2Q was added, the photocurrent increased (curve 3). These results indicated that both I^- and H_2Q contributed equally to the photoanodic reactions at MoS_2 in CH_3CN. This is in a marked contrast to the results in an aqueous electrolyte (Fig. 6(A)). Schneemeyer and Wrighton[17] also reported that Cl^- ions could be efficiently photo-oxidized at n-MoS_2 in CH_3CN.

Photoelectrochemical Reactions at p-MoS_2 Electrode. We confirmed that the cathodic reaction at the p-MoS_2 electrode was the following process,

$$2H^+ + 2e^- \longrightarrow H_2, \quad (4)$$

and the onset of the photocurrent was shifted to a more negative potential with an increase in the pH. This was because the hydrogen overvoltage was heightened, *i.e.*, $E_{onset}=-0.2$ V *vs.* SCE(in 0.5 M H_2SO_4), -0.5 V (in 0.1 M KCl), and -0.8 V (in 1 M NaOH). The onset of the photocurrent was more negative than the flatband potential. This indicates that the recombination of photogenerated electron-hole pair occurs at the small cathodic band bending.

Figure 8 shows the current-potential curves of Pt ring/p-MoS_2 disk RRDE with Fe^{3+} as the oxidizing agent. The Pt ring potential (E_R) was held at 1.0 V *vs.* SCE to detect the oxidation current (I_R) of the Fe^{2+} ions produced at the MoS_2 disk electrode. In the absence of Fe^{3+} ions, no ring current could be observed (lower portion of Fig. 8, curve 1). This indicated that the current at the MoS_2 disk in the presence or absence of light (upper portion of Fig. 8, curve 1) was due to the process (4). In the presence of the Fe^{3+} ions, the onset of the photocurrent was shifted to a more positive potential and a ring current could be observed (curves 2 and 3). Shifts in the onset of the photocurrent could also be observed with the addition of other oxidizing agents such as quinone and $Fe(CN)_6^{3-}$. This phenomenon seems to be the

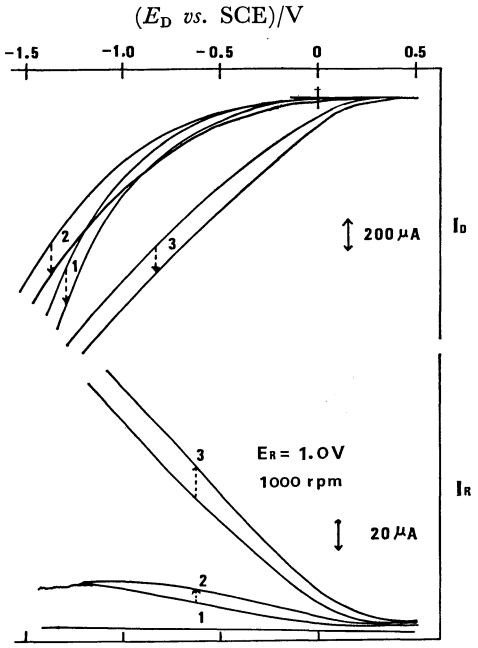

Fig. 8. I_R-E_D, I_D-E_D curves of Pt ring/p-MoS_2 disk electrode in 0.5 M H_2SO_4 solutions with different concentrations of Fe^{3+} ions. The rotation speed was 1000 min^{-1}.
1: 0 M, 2: 5×10^{-3} M, 3: 10^{-1} M.

same as in the case of n-MoS_2 electrode in I^- solutions. However, in the case of p-MoS_2, its flatband potential is not changed by the addition of oxidizing agents, for the photocurrent at the potential more positive than −0.2 V may be resulted from the process that the electron transfer from MoS_2 to Fe^{3+} is faster than the recombination of an electron-hole pair.

Figure 9 shows the ratio of the competitive electron capture by the Fe^{3+} ions to that by the H^+ ions as a function of the Fe^{3+} concentration. At E=0 V, the ratio was 1 and was independent of the Fe^{3+} concentration. This revealed that the photocurrent at 0 V was entirely due to the reduction of Fe^{3+} ions. At more cathodic potential (−0.8 V), the photocurrent was due to the competitive reduction of the Fe^{3+} ions and the hydrogen formation reaction, thus the higher the Fe^{3+} concentration, the more the hydrogen formation reaction was suppressed, and thus the larger was the ratio. Again, electron capture by the Fe^{3+} ions was 100% when the Fe^{3+} concentration was 10^{-2} or higher.

Conclusion

The MoS_2 photoanode was remarkably stabilized in I^- solutions. This effect may be attributed to the specific adsorption of I^- ions on the electrode surface, and the adsorption sites may act as surface states which participated in charge transfer. The ratios of the competitive oxidation of other reducing agents studied were very small (less than 20% hole capture), and hence they were not suitable for the stabilization of the MoS_2 photoanode. The competitive oxidations of the reducing agents were not clearly dependent on their redox potential. This was in a sharp contrast

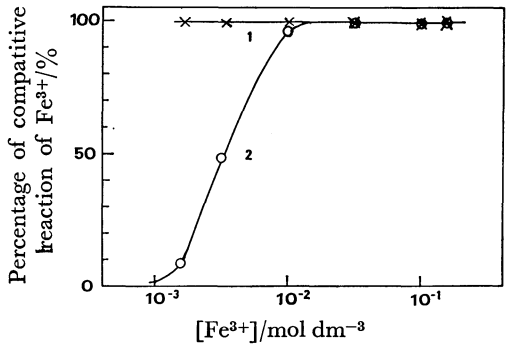

Fig. 9. Dependence of the percentage of competitive reaction of Fe^{3+} at the p-MoS_2 electrode on Fe^{3+} at two different potentials, and at constant light intensity and rotation speed.
1: E=0 V, 2: E=−0.8 V.

to that at a CdS photoanode. The cathodic reaction at the p-MoS_2 electrode was the hydrogen formation process. The onset of the photocurrent shifted in the presence of oxidizing agents. This fact may be resulted from the process that the electron transfer across the semiconductor-solution interface is faster than the recombination of an electron-hole pair.

References

1) J. A. Woollam and R. B. Somoano, *Phys. Rev. B*, **13**, 3843 (1976).
2) D. W. Murphy and F. A. Trumbore, *J. Cryst. Growth*, **39**, 185 (1977).
3) H. Tributsch and J. C. Bennett, *J. Electroanal. Chem.*, **81**, 97 (1977).
4) H. Tributsch, *Ber. Bunsenges. Phys. Chem.*, **81**, 361 (1977).
5) H. Tributsch, *J. Electrochem. Soc.*, **125**, 1086 (1978).
6) J. Gobrecht, H. Tributsch, and H. Gerischer, *J. Electrochem. Soc.*, **125**, 2085 (1978).
7) J. Gobrecht, H. Gerischer, and H. Tributsch, *Ber. Bunsenges. Phys. Chem.*, **82**, 1331 (1978).
8) S. M. Ahmed and H. Gerischer, *Electrochim. Acta*, **24**, 705 (1979).
9) W. Kautek, H. Gerischer, and H. Tributsch, *Ber. Bunsenges. Phys. Chem.*, **83**, 1000 (1979).
10) H. Tributsch, H. Gerischer, C. Clemen, and E. Bucher, *Ber. Bunsenges. Phys. Chem.*, **83**, 655 (1979).
11) W. Kautek and H. Gerischer, *Ber. Bunsenges. Phys. Chem.*, **84**, 645 (1980).
12) W. Kautek, H. Gerischer and H. Tributsch, *J. Electrochem. Soc.*, **127**, 247 (1980).
13) H. J. Lewerenz, A. Heller, and F. J. DiSalvo, *J. Am. Chem. Soc.*, **102**, 1877 (1980).
14) S. Menezes, F. J. DiSalvo, and B. Miller, *J. Electrochem. Soc.*, **127**, 1751 (1980).
15) L. F. Schneemeyer and M. S. Wrighton, *J. Am. Chem. Soc.*, **102**, 6496 (1979).
16) C. P. Kubiak, L. F. Schneemeyer, and M. S. Wrighton, *J. Am. Chem. Soc.*, **102**, 6898 (1980).
17) L. F. Schneemeyer and M. S. Wrighton, *J. Am. Chem. Soc.*, **102**, 6964 (1980).
18) L. F. Schneemeyer, M. S. Wrighton, A. Stacy, and M. J. Sienko, *Appl. Phys. Lett.*, **36**, 701 (1980).
19) F. R. Fan, H. S. White, B. Wheeler, and A. J. Bard, *J. Electrochem. Soc.*, **127**, 518 (1980).
20) F. R. Fan, H. S. White, B. Wheeler, and A. J. Bard,

J. Am. Chem. Soc., **102**, 5142 (1980).
21) D. Canfield and B. A. Parkinson, *J. Am. Chem. Soc.*, **103**, 1279 (1981).
22) B. A. Parkinson, T. E. Furtak, D. Canfield, K. Kam, and G. Kline, *Discuss. Faraday Soc.*, **70**, 233 (1980).
23) G. Kline, K. Kam, D. Canfield, and B. A. Parkinson, *Solar Energy Mat.*, **4**, 301 (1981).
24) T. Inoue, T. Watanabe, A. Fujishima, and K. Honda, *J. Electrochem. Soc.*, **124**, 719 (1977).
25) T. Biegler and D. A. Swift, *Electrochim. Acta*, **24**, 415 (1979).
26) J. Lagrenaudie, *J. Phys. Radium*, **15**, 299 (1954).
27) R. F. Frindt and A. D. Yoffe, *Proc. R. Soc. London, Ser. A*, **273**, 69 (1962).
28) A. J. Bard, *J. Photochem.*, **10**, 59 (1979).
29) T. Inoue, T. Watanabe, A. Fujishima, and K. Honda, *Bull. Chem. Soc. Jpn.*, **52**, 1243 (1979).
30) H. Minoura and M. Tsuiki, *Electrochim. Acta*, **23**, 1377 (1978).
31) T. Inoue, A. Fujishima, and K. Honda, *Bull. Chem. Soc. Jpn.*, **52**, 3217 (1979).
32) A. Fujishima, T. Inoue, and K. Honda, *J. Am. Chem. Soc.*, **101**, 5582 (1979).